HHS Public Access

Author manuscript

Ann N Y Acad Sci. Author manuscript; available in PMC 2020 April 01.

Published in final edited form as:

Ann N Y Acad Sci. 2019 April ; 1442(1): 79–90. doi:10.1111/nyas.13914.

Role of pannexin 1 channels in load-induced skeletal response

Zeynep Seref-Ferlengez[1,5], **Marcia Urban-Maldonado**[1,2], **Herb B. Sun**[1,4,5], **Mitchell B. Schaffler**[6], **Sylvia O. Suadicani**[2,3], and **Mia M. Thi**[*,1,3,5]

[1]Department of Orthopedic Surgery, Albert Einstein College of Medicine and Montefiore Medical Center, Bronx, NY

[2]Department of Urology, Albert Einstein College of Medicine and Montefiore Medical Center, Bronx, NY

[3]Department of Neuroscience, Albert Einstein College of Medicine and Montefiore Medical Center, Bronx, NY

[4]Department of Radiation Oncology, Albert Einstein College of Medicine and Montefiore Medical Center, Bronx, NY

[5]Laboratories of Musculoskeletal Orthopedic Research at Einstein-Montefiore (MORE), Albert Einstein College of Medicine and Montefiore Medical Center, Bronx, NY

[6]Department of Biomedical Engineering, City College of New York, NY

Abstract

The pannexin 1 (Panx1) channel is a mechanosensitive channel that interacts with P2X7 receptors (P2X7R) to form a functional complex that has been shown *in vitro* to play an essential role in osteocyte mechanosignaling. While the participation of P2X7R in skeletal responses to mechanical loading has been demonstrated, the role of Panx1 and of its interplay with P2X7R still remain to be determined. In this study, we use a global *Panx1*$^{-/-}$ knockout mouse model and *in vivo* mechanical loading to demonstrate for the first time that Panx1 channels play an essential role in load-induced skeletal responses. We found that absence of Panx1 not only disrupts the P2X7R-Panx1 signaling complex, but also alters load-induced regulation of P2X7R expression. Moreover, lack of Panx1 completely abolished load-induced periosteal bone formation. Load-induced regulation of β-catenin and sclerostin expression was dysregulated in *Panx1*$^{-/-}$ compared to wildtype bone. This finding suggests that Panx1 deficiency disrupts Wnt/β-catenin signaling by lowering β-catenin while favoring inhibition of bone formation by increasing load-induced sclerostin expression. In sum, this study demonstrates the existence of a Panx1-dependent mechanosensitive mechanism that not only modulates ATP signaling but also coordinates Wnt/β-catenin signaling that is essential for proper skeletal response to mechanical loading.

Address for correspondence: Mia M. Thi, Ph.D., Department of Orthopaedic Surgery, Albert Einstein College of Medicine, 1300 Morris Park Avenue, Kennedy Center, Rm 812, Bronx, NY 10461. mia.thi@einstein.yu.edu.

Competing Interests

The authors declare no competing interests.

Keywords

mechanical loading; Panx1; osteocytes; β-catenin; sclerostin

Introduction

Bone is well recognized as an intricate mechanosensitive organ. Mechanical loading is essential for maintaining bone health, as clearly demonstrated by marked bone dysfunction associated with unloading due to space flight or bed rest.[1, 2] Adaptation to mechanical loading throughout life is important for developing the proper skeleton and maintaining its integrity. Osteocytes, the most abundant cells in bone, sense and integrate both mechanical and chemical signals from their environment, and initiate and coordinate the responses of the effector cells (osteoblasts and osteoclasts) that are required for local regulation of both bone formation and resorption.[3–5] Although the role of osteocytes as key mechanosensors has become well-accepted, the mechanisms and molecular mediators that account for their cellular mechanobiology are not completely understood. A series of recent studies by our group has demonstrated that there is a unique mechanosensory complex in osteocytes consisting of pannexin 1 channel (Panx1), purinergic P2X7 receptor (P2X7R), αVβ3 integrin, and T-type calcium channel CaV3.2-1.[6–8]

Panx1, one of the key components of this complex, is a member of the gap junction family of proteins that forms large non-junctional channels that allow diffusion of ions and small molecules (<1 kDa) between the cytosol and extracellular space. Besides being activated by P2X7R and other purinergic P2 receptors, Panx1 channels are sensitive to voltage, high extracellular K^+, and mechanical stimulation.[9–11] Panx1 is expressed in various cell types and has been shown to participate in key cellular events, such as intercellular signaling, mechanotransduction, and inflammatory responses.[7, 12–17] Studies by us and others have shown that Panx1 and P2X7R play essential roles in controlled cellular release of signaling molecules such as ATP, Ca^{2+}, PGE_2, and IL-1β in response to mechanical or chemical stimulation,[7, 14, 15, 18–22] and participate in many physiological and pathological processes.[23–30] Moreover, we have shown that Panx1 and P2X7R form a functional complex in osteocytes that plays a key role in osteocyte mechanosignaling and in apoptotic signaling by providing a major pathway for ATP release.[7, 30]

A recent study has shown that absence of Panx1 results in β-catenin downregulation in melanoma cells.[31] β-catenin is an important component of the canonical Wnt signaling pathway that is well recognized for its critical role in bone homeostasis; the activation of this pathway leads to increased bone mass and strength, while its inhibition results in decreased bone integrity.[32, 33] This signaling pathway is activated by binding of canonical Wnt ligands to a dual receptor complex consisting of the Wnt co-receptors Lrp5 or Lrp6 (Lrp5/6) and one of the Frizzled family of seven-transmembrane receptors.[33] Formation of this receptor complex results in inactivation of the multiprotein β-catenin complex through which the main signaling mediator β-catenin is released from its constitutive proteosomal degradation, leading to β-catenin accumulation in the cytoplasm.[34] This leads to nuclear translocation of

β-catenin where further interaction with transcription factors transactivates the transcription target genes responsible for bone homeostasis.[33]

Moreover, additional insight into the Wnt/β-catenin signaling from various studies have clearly demonstrated its essential role not only in skeletal mechanotransduction and load-induced anabolic response in bone,[35–39] but also as a pathway whereby osteocytes transmit mechanosignals.[34, 40–44] Mounting evidence shows that osteocyte-derived Wnt antagonists are negative regulators of bone mass.[32, 33] Sclerostin, a glycoprotein secreted by mature osteocytes, inhibits Wnt/β-catenin signaling by binding to the Wnt co-receptors Lrp5, Lrp6, or both.[45–47] Some of the most compelling evidence supporting the role of sclerostin in bone mechanobiology comes from studies demonstrating that mechanical loading suppresses osteocyte sclerostin secretion and thus favors Wnt/β-catenin signaling-dependent bone anabolic response.[44, 48]

The role of Panx1 channels in osteocyte mechanosignaling and its functional interplay with P2X7R has been determined *in vitro*.[7] However, while the role of P2X7R in skeletal mechanoresponsiveness[18] has been demonstrated, the importance of Panx1 in these responses and the potential interaction of Panx1 signaling with the Wnt/β-catenin signaling have not been investigated. In this study we thus used global Panx1-null and wildtype mice, an *in vivo* mechanical loading paradigm (treadmill loading), dynamic bone histomorphometric analysis, real time quantitative PCR, and western blotting analyses to determine the extent to which the absence of Panx1 impacts skeletal responses to mechanical loading.

Materials and Methods

Animals

Age-matched male 10–12-week-old Panx1-null (*Panx1*$^{-/-}$) mice and wildtype male C57BL/6NCrl mice were used in this study. The *Panx1*$^{-/-}$ mice on the C57BL/6NCrl background were generated in our animal facility by breeding heterozygous Panx1$^{tm1a(KOMP)Wtsi}$ purchased from the Knockout Mouse Project (KOMP; www.KOMP.org).[22, 49] We have shown that *Panx1* mRNA expression in *Panx1*$^{-/-}$ mice is reduced by 70% compared to wildtype (*Panx1*$^{+/+}$) mice,[49] but these mice are functional *Panx1* knockouts.[26] Wildtype C57BL/6NCrl mice were purchased from Charles River Laboratories and bred and maintained in our animal facility. All mice were allowed free access to standard mouse chow and water during the entire experimental period. Animals were treated in strict accordance with the National Institutes of Health (NIH) animal care guidelines and experimental procedures were approved by the Einstein Animal Care and Use Committee (IACUC approval number: 20150602). We chose to use young adult mice in this study to allow investigating the role of Panx1 during a critical time window for skeletal growth that once altered may result in substantial lifelong effects on skeletal health.[50]

Mechanical loading paradigm

Panx1$^{-/-}$ and control wildtype (WT) mice were exposed to a treadmill loading paradigm as follows: mechanical loading group and cage control group (4–6 mice per group). The

mechanical loading group was subjected to treadmill running for 2 or 4 weeks (5 days/wk, total of 300 meters/day, speed up to 10 meter/min at a 5° incline using Columbus Instruments, Model 1055M, Columbus, OH).[51, 52] All mice were allowed normal cage activity between loading sessions. Intraperitoneal injections of calcein (30 mg/kg body weight, Sigma-Aldrich, St. Louis, MO) were administered 3 and 10 days after the first loading day for the 2-week loading group and their cage control group. The cage control and loaded animals were euthanized immediately after the last running bout.

Tissue collection

Both hindlimbs and forelimbs were harvested after animals were euthanized. Right femurs were fixed in 10% neutral buffered formalin (Fisher Scientific, PA) and processed for histomorphometry studies as detailed below. The diaphyses of femora, tibiae, humeri, radii and ulnae were cleaned of soft tissues and the marrow was flushed out with 1× PBS (except radii and ulnae) to yield osteocyte-enriched samples, as previously described.[7, 30, 53, 54] Samples were homogenized (Sartorius Mikro-Dismembranator, Germany) and protein or RNA was extracted. Left hindlimbs were used to examine protein expression by western blotting. Forelimbs were used to examine mRNA expression by qPCR.

Western blotting

Tissue samples were sonicated in lysis buffer (5 mM EDTA, 1 mM sodium orthovanadate, 1 mM $NaHCO_3$, 2 mM PMSF [Sigma-Aldrich], and 1× protease inhibitor [Roche, Mannheim, Germany]), electrophoresed on 10% SDS-PAGE gels for separation, and then transferred to nitrocellulose membranes (Whatman GmbH, Dassel, Germany). The membranes were probed with primary polyclonal antibodies to P2X7R (1:1000; APR-004, Alomone Labs, Israel), Panx1 (N [Term], 1:100; Cat 487900, Invitrogen Corporation, CA), and β-actin (1:35000; A1978, Sigma-Aldrich), followed by incubation with the respective horseradish peroxidase (HP)-conjugated anti-rabbit IgG or anti-mouse IgG (1:10000; Santa Cruz Biotechnology, TX) antibody. The protein bands were detected with the In Vivo FX PRO imaging system (Carestream, NY) using the Immobilon western detection kit (Millipore, MA), as previously described.[7] Densitometric analyses were performed using ImageJ (NIH) software. Measured intensities for all samples were first normalized with the respective β-actin loading control, and then with either the age-matched non-loaded WT or the age-matched non-loaded *Panx1*$^{-/-}$ bone tissue samples.

Real-time quantitative PCR (qPCR)

qPCR was used to compare mRNA expression levels of β-catenin (*Ctnnb1*) and sclerostin (the *Sost* gene product) in non-loaded and loaded WT and *Panx1*$^{-/-}$ bones. Total RNA was extracted using TRIzol reagent (Invitrogen) and qPCR was performed using SYBR GREEN Master Mix (Applied Biosystems, CA) in an Applied Biosystems 7300 Real-Time PCR System (Forester City, CA), according to the manufacturer's instructions and as previously described.[55] Briefly, 0.5 μg of total RNA was reverse transcribed into cDNA using SuperScript VILO (Invitrogen). RT reactions were diluted in RNase-free water in a 1:50 ratio and 3 μl of this dilution was used in amplification reactions carried out for 40 cycles with annealing temperature of 60°C in a 25μl of final volume. Finally, a dissociation profile of the PCR product(s) was obtained by a temperature gradient running from 60°C to 95°C.

Forward and reverse primer sequences were: *Ctnnb1*: forward TTAAACTCCTGCACCCACCAT/ reverse AAGGGCAAGGTTTCGAATCA (Primer Express, Applied Biosystems); *Sost*: forward GGAATGATGCCACAGAGGTCAT / reverse CCCGGTTCATGGTCTGGTT;[56] *18S*: forward CACGGCCGGTACAGTGAAAC / reverse AGAGGAGCGAGCGACCAAA.[57] We performed two technical replicates for each experiment, with a total of four biological replicates for each set of samples. Relative gene expression levels of the mRNA analyzed were calculated using the delta-delta CT method, where values obtained for the gene of interest are first normalized to those of the reference gene (18S rRNA gene) and subsequently to those of their respective age-matched controls (non-loaded WT or non-loaded *Panx1*$^{-/-}$).

Histomorphometric Analysis

The femurs were stained en-bloc with Villanueva staining, dehydrated by a graded ethanol series, and embedded undecalcified in poly-methyl methacrylate (PMMA), as previously described.[58] Cross-sections from the mid-diaphysis were cut using a diamond wafering saw (Leica SP1600 microtome, Leica Biosystems, IL). Sections were polished to 90 μm and two sections per femur were examined using OsteoMeasure (OsteoMetrics, GA) in a Zeiss microscope (Carl Zeiss, CA) with 10× objective. Total perimeter (B.Pm), single label perimeter (sL.Pm), double label perimeter (dL.Pm), double label area (dL.Ar), and interlabeled width (Ir.L.Wi [μm]) were measured from periosteal (Ps) and endocortical (Ec) surfaces. Cortical bone area (Ct.B.Ar, [mm^2]), total area (Tt.Ar, [mm^2]), marrow area (Ma.Ar, [mm^2]), cortical thickness (Ct.Th, [μm]), polar moment of inertia (*J*, [mm^4]) and area moment inertia (I_x and I_y, [mm^4]) were also measured. The following parameters were calculated as previously described: mineralizing surface (MS/BS [%]: [(sL.Pm+dL.Pm)/ 2B.Pm]×100%); mineral apposition rate (MAR [μm/day]: Ir.L.Wi/7); bone formation rate (BFR/BS [μm^3/μm^2/day]: MARxMS/BS).[59, 60] Measurements were made by a single observer (ZS-F) who was blinded to specimen identification.

Statistical analysis

Data were analyzed from four to seven independent sets of experiments using ImageJ (NIH) and Prism 7 software (GraphPad, CA). Statistical differences between different loaded and non-loaded samples were determined by one-way ANOVA followed by Tukey's multiple comparison test, or by an unpaired *t*-test followed by Mann-Whitney comparison test. $P < 0.05$ was considered statistically significant.

Results

Effect of mechanical loading on Panx1 and P2X7R expression in bone

In our previous *in vitro* and *in situ* studies, we demonstrated that Panx1 and P2X7R form a functional complex and play an important role in osteocyte mechanosignaling, which is essential for proper bone homeostasis.[5, 7, 61] In this study, we now demonstrate that *in vivo* mechanical loading modulates Panx1 and P2X7R expression in osteocyte-enriched wildtype bone tissue, which not only changes in response but also adapts to different loading durations. In the initial 2-week loading phase, we observed significant upregulation of Panx1 and P2X7R expression in the wildtype loaded bone compared to non-loaded control, as

shown in Figure 1 (white bars). By the end of the 4-week loading bout, both Panx1 and P2X7R levels in loaded wildtype bone tissue are comparable to that of the non-loaded control, likely indicating that bone has fully adapted to the loading paradigm (Fig. 1, gray bars). However, this adaptive response was absent in the *Panx1*$^{-/-}$ bone tissue. As shown in Figure 2, P2X7R expression is unchanged in response to mechanical loading in *Panx1*$^{-/-}$ bone, especially at the 2-week loading time point, when compared either to non-loaded age-matched wildtype (Fig. 2A, green bar with hollow circles) or to non-loaded age-matched *Panx1*$^{-/-}$ (Fig. 2B, green bar with solid triangles).

Load-induced bone formation in Panx1$^{-/-}$ mice

We found that young adult *Panx1*$^{-/-}$ mice seem skeletally normal compared to age-matched wildtype mice. No apparent differences in body weight, Ma.Ar, Ct.Th, polar moment of inertia, or area moment of inertia were noted between non-loaded *Panx1*$^{-/-}$ and non-loaded wildtype mice at 12 weeks of age (Table 1). Some of the femoral midshaft parameters, however, were significantly larger in *Panx1*$^{-/-}$ mice when compared to age-matched wildtype mice (Tt.Ar [~10%] and Ct.B.Ar [~19%]). We found that wildtype mice responded to mechanical loading with a significant increase in Tt.Ar (13%), Ct.B.Ar (16%), Ma.Ar (13%), J (31%), I_x (25%) and I_y (30%), indicating an anabolic response (radial expansion) after 4 weeks of loading (see Table 1, shaded in light gray). In contrast, load-induced anabolic response was largely absent in *Panx1*$^{-/-}$ mice (Table 1). In addition to the lack of load-induced anabolic response, the *Panx1*$^{-/-}$ mice displayed significant reduction in Tt.Ar (−7%) and Ct.B.Ar (−14%) (Table 1, shaded in medium gray).

At the 2-week loading time point, when higher expression of Panx1 and P2X7R expression was observed in wildtype mice, dynamic histomorphometric analysis was performed to compare the bone formation activities in wildtype and Panx1$^{-/-}$ mice. As shown in Figure 3 and Table 2, mechanical loading significantly increased periosteal mineralizing surface and bone formation rate of wildtype femurs relative to that of non-loaded controls (Ps.MS/BS = 29.9% vs. 17.5%; Ps.BFR/BS = 0.47 $\mu m^3/\mu m^2$/day vs. 0.25 $\mu m^3/\mu m^2$/day), whereas it induced a marked reduction in the periosteal mineralizing surface and bone formation rate in loaded *Panx1*$^{-/-}$ femurs compared to non-loaded *Panx1*$^{-/-}$ controls (Ps.MS/BS = 23.7% vs 15.5%; Ps.BFR/BS = 0.20 $\mu m^3/\mu m^2$/day vs. 0.34 $\mu m^3/\mu m^2$/day). Mineral apposition rates on both periosteal and endocortical surfaces were similar in wildtype and *Panx1*$^{-/-}$ mice regardless of mechanical loading. In addition, no statistical differences were observed in endocortical mineralizing surface between loaded and non-loaded bones in both wildtype and *Panx1*$^{-/-}$ mice.

Load-induced Wnt/β-catenin signaling in Panx1$^{-/-}$ mice

The Wnt/β-catenin signaling is essential for skeletal mechanotransduction and load-induced anabolic responses in bone.[35–38] The effect of loading on mRNA expression levels of β-catenin (*Cnntb1*) and sclerostin (*Sost*) in osteocyte-enriched bone was compared between wildtype and *Panx1*$^{-/-}$ bones. We found that at the end of 4-week loading bout, when wildtype mice have fully adapted to the loading (see Fig.1) and the load-induced bone formation is apparent (Tables 1 and 2 and Fig. 3), mRNA expression of load-induced β-catenin and sclerostin levels were similar to those of non-loaded wildtype (Fig. 4A and B,

blue bars with hollow circles). However, load-induced relative β-catenin mRNA expression in *Panx1*$^{-/-}$ bones was significantly lower compared either to that of non-loaded wildtype (Fig. 4A, pale red bars with hollow squares) or non-loaded *Panx1*$^{-/-}$ (Fig. 4A, pale red bar with hollow triangles). In contrast, load-induced sclerostin mRNA expression in Panx1$^{-/-}$ bones was subtly yet significantly higher than that of their age-matched non-loaded wildtype bones (Fig. 4B, pale red bars with hollow squares) and non-loaded *Panx1*$^{-/-}$ bones (Fig. 4B, pale red bar with hollow triangles).

Discussion

Previous studies have clearly demonstrated the many faceted roles played by Panx1 as a mechanosensitive channel, a conduit for ATP release, and as a key mediator in mechanisms of intercellular signaling and in inflammatory responses.[12, 13, 15, 17] However, the role of these channels in the regulation of bone mechanosignaling is still emerging. Although the participation of Panx1 in osteocyte mechanosignaling has been strongly supported by *in vitro* studies,[7] it has yet to be verified in depth in an *in vivo* context. In this study we used a global knockout mouse model to demonstrate for the first time that Panx1 channels play an essential role in load-induced skeletal responses.

In previous *in vitro* studies with an osteocyte cell line we showed that Panx1 forms a unique mechanosignaling complex with P2X7R and that it acts as a conduit for flow-induced ATP release.[7] We have now demonstrated that *in vivo* mechanical loading regulates both Panx1 and P2X7R expression in osteocyte-enriched wildtype bones in a loading time–dependent manner, with higher expression levels at 2 weeks after loading (Fig. 1, white bars) and returning to control levels after 4 weeks of loading, when the adaptive response to loading has likely been attained (Fig. 1, gray bars). This load-induced modulation of P2X7R response was lost in the absence of Panx1 (Fig. 2). These findings strongly demonstrate the existence of a functional interplay and load-induced regulation of the P2X7R-Panx1 signaling complex that is critical for proper osteocyte mechanosignaling. In addition, our current data indicates that absence of Panx1 would not only disrupt the P2X7R-Panx1 signaling complex, but also impair load-induced regulation of P2X7R expression. From a functional standpoint, disruption of the P2X7R-Panx1 complex would blunt load-induced ATP release and the feed-forward mechanism of ATP-induced ATP release that amplifies load-induced intercellular signaling within the osteocytic network, as we have previously proposed,[62] and thereby impact overall bone responses to loading.

This hypothesis is supported by our findings that load-induced bone anabolic response, specifically periosteal bone formation, is completely abolished in *Panx1*$^{-/-}$ mice. The osteogenic response (bone formation rate [BFR], mineralizing surface [MS/BS]) on the periosteal surface was the most affected by the lack of Panx1 (Tables 1 and 2 and Fig. 3). Our observation that mineral apposition rate (MAR), which represents the activity of a group of osteoblasts,[60] is not affected by the loss of Panx1 suggest that load-induced osteoblast activity in Panx1$^{-/-}$ mice is relatively the same as that in wildtype mice. However, BFR, which is influenced by the rate of bone remodeling activation (i.e. depends on the number of osteoblast groups and on their coordinated activity),[60] is greatly affected by the lack of Panx1, which strongly indicates that load-induced bone remodeling activation is blunted. In

other words, in the absence of Panx1, the load-induced activity of osteoblast clusters is reduced likely due to inability of osteocytes to communicate and coordinate loading signals with osteoblasts and, thereby, to properly regulate the anabolic response. Although no apparent differences in skeletal phenotype (femora diaphyseal structure) has been reported between adult *Panx1*$^{-/-}$ and wildtype mice,[30] in our current studies we observed a slight but notably larger femoral midshaft (only in Tt.Ar and Ct.B.Ar) in young adult *Panx1*$^{-/-}$ when compared to their age-matched wildtype counterparts (Table 1). Similar findings were recently reported in preliminary studies presented at a conference, in which young adult mice with a targeted, osteocyte-specific *Panx1* deletion were shown to display significantly higher bone mass and femoral cortical thickness than wildtype mice.[63] Moreover, the authors observed reduced osteoclastic parameters in these mice, which led them to propose that lack of osteoclastogenic signals from Panx1-deficient osteocytes would contribute to the observed higher cortical bone parameters in young mice.[63] It has to be mentioned, however, that no activation of either intracortical resorption or endocortical tunneling resorption was observed under fatigue loading conditions in mice with a global *Panx1* deletion (Panx1$^{-/-}$) when compared to their wildtype counterparts.[30] These findings further highlight the complexity of the role of Panx1 in bone homeostasis.

The participation of P2X7R in load-induced anabolic responses is well recognized.[18] Bone mechanoresponsiveness was reported to be reduced to ~73% in the absence of P2X7R.[18] Nonetheless, we observed that absence of Panx1 completely abolished the load-induced bone response, which strongly suggests that the role of Panx1 in bone mechanosignaling and transduction may be even more critical than that of P2X7R. It has to be noted that mice on the C57BL/6 background harbor a single amino-acid mutation (P451L) on the P2X7R cytoplasmic tail that renders the receptor still capable of performing as a cation channel but largely attenuates pore formation.[64] In a previous study we addressed the overall impact that this mutation has on the functional interplay between P2X7R and Panx1.[65] Our electrophysiological, biochemical, pharmacological, and fluorescence imaging data revealed that the P451L mutation significantly attenuates Panx1 currents, ATP release, and the range of intercellular calcium signaling between astrocytes. One would expect that a similar attenuation of the P2X7R-Panx1 mediated signaling would be observed in C57BL/6 bones when compared to bones of mice with the non-mutated P2X7R. In this regard, by having to use C57BL/6 in the present studies and to compare findings from *Panx1*$^{-/-}$ mice against those of wildtype mice with already reduced P2X7R-Panx1 function, we are likely underestimating the full impact of *Panx1* deletion on load-induced bone response. Collectively, our observation that load-induced anabolic responses are accompanied by adaptive regulation of P2X7R-Panx1 expression in wildtype bones, which are lost in *Panx1*$^{-/-}$ bones, emphasizes the essential role for this mechanosignaling complex in proper bone homeostasis.

It has been shown that deletion of *Panx1* downregulates β-catenin expression in melanoma cells.[31] β-catenin is an important player in the Wnt signaling pathway that is essential for skeletal mechanotransduction and load-induced anabolic response in bone.[35–37] Osteocytes use the Wnt/β-catenin signaling pathway as one of the means to transmit mechanosignals within the bone cell-network,[34, 39–43] and secrete sclerostin, a negative regulator of Wnt/β-catenin signaling that inhibits bone formation.[32, 33, 46] However, a possible link between

Panx1 and Wnt/β-catenin signaling in the bone, particularly in response to mechanical loading, has yet to be demonstrated. We observed that β-catenin expression in non-loaded $Panx1^{-/-}$ osteocyte-enriched bones is slightly but not significantly lower than that in non-loaded wildtype bones (Fig. 4), which indicates that under basal conditions the absence of Panx1 does not affect Wnt/β-catenin signaling. However, our findings that mechanical loading significantly downregulates β-catenin and upregulates sclerostin in $Panx1^{-/-}$ bones when compared to wildtype bones (Fig. 4) indicates the existence of crosstalk between Panx1 and Wnt/β-catenin signaling that is critical to achieve proper load-induced bone adaptation. Under normal conditions, mechanical loading reduces *Sost* transcription and sclerostin protein expression,[44] and activates β-catenin signaling in osteocytes,[34, 39, 43] which favor bone formation. Our findings suggest that absence of Panx1 disrupts this normal load-induced regulation of Wnt/β-catenin signaling in osteocytes by increasing sclerostin, which in turn would antagonize Wnt signaling by interacting with Lrp5/6 and thereby inhibit Wnt binding and signaling through its receptor complex. In this scenario, in the absence of Wnt signaling, the β-catenin levels will be markedly reduced because of its constitutive proteosomal degradation[33, 34], and would thereby favor inhibition of bone formation.

In summary, this study demonstrates for the first time the critical role of Panx1 in load-induced skeletal responses. Most importantly, it discloses the existence of a Panx1-dependent mechanosensitive mechanism that regulates the expression of the P2X7R-Panx1 signaling complex as well as expression of both β-catenin and sclerostin in bone. Through this mechanism, Panx1 would play a central role in modulating not only ATP signaling but also in coordinating the load-induced Wnt/β-catenin signaling that is essential for proper skeletal response to mechanical loading.

Acknowledgments

This work was supported by the National Institutes of Health National Institute of Diabetes and Digestive and Kidney Disease under Award Number DK091466 (to MMT, SOS and ZS), National Institute of Arthritis and Musculoskeletal and Skin Diseases under award numbers (AR073475 to MMT and SOS), and equipment from a shared instrumentation grant from the National Institutes of Health under Award Number S10 RR020949. The content is solely the responsibility of the authors and does not necessarily represent the official views of the National Institutes of Health. Author contributions: ZS, SOS and MMT designed research; ZS, MU, SOS and MMT performed research; HBS, MBS, SOS, MMT contributed reagents and analytic tools; ZS, MU and MMT analyzed data; SOS and MMT wrote the paper; ZS, MU, HBS, SOS, and MMT edited the paper.

References

1. Robling AG, Hinant FM, Burr DB, et al. 2002; Improved bone structure and strength after long-term mechanical loading is greatest if loading is separated into short bouts. J. Bone Miner. Res. 17:1545–1554. [PubMed: 12162508]
2. Robling AG, Castillo AB, Turner CH. 2006; Biomechanical and molecular regulation of bone remodeling. Annual review of biomedical engineering. 8:455–498.
3. Aarden EM, Burger EH, Nijweide PJ. 1994; Function of osteocytes in bone. J. Cell. Biochem. 55:287–299. [PubMed: 7962159]
4. Bellido T. 2014; Osteocyte-driven bone remodeling. Calcif. Tissue Int. 94:25–34. [PubMed: 24002178]
5. Schaffler MB, Cheung WY, Majeska R, et al. 2014; Osteocytes: master orchestrators of bone. Calcif. Tissue Int. 94:5–24. [PubMed: 24042263]

6. Cabahug-Zuckerman P, Stout RF Jr, Majeska RJ, et al. 2018; Potential role for a specialized beta3 integrin-based structure on osteocyte processes in bone mechanosensation. J. Orthop. Res. 36:642–652. [PubMed: 29087614]
7. Seref-Ferlengez Z, Maung S, Schaffler MB, et al. 2016; P2X7R-Panx1 Complex Impairs Bone Mechanosignaling under High Glucose Levels Associated with Type-1 Diabetes. PLoS One. 11:e0155107. [PubMed: 27159053]
8. Thi MM, Suadicani SO, Schaffler MB, et al. 2013; Mechanosensory responses of osteocytes to physiological forces occur along processes and not cell body and require alphaVbeta3 integrin. Proc. Natl. Acad. Sci. U. S. A. 110:21012–21017. [PubMed: 24324138]
9. Penuela S, Gehi R, Laird DW. 2013; The biochemistry and function of pannexin channels. Biochim. Biophys. Acta. 1828:15–22. [PubMed: 22305965]
10. Scemes E, Spray DC, Meda P. 2009; Connexins, pannexins, innexins: novel roles of "hemi-channels". Pflugers Arch. 457:1207–1226. [PubMed: 18853183]
11. Sandilos JK, Bayliss DA. 2012; Physiological mechanisms for the modulation of pannexin 1 channel activity. J. Physiol. 590:6257–6266. [PubMed: 23070703]
12. Suadicani SO, Iglesias R, Wang J, et al. 2012; ATP signaling is deficient in cultured Pannexin1-null mouse astrocytes. Glia. 60:1106–1116. [PubMed: 22499153]
13. Bao L, Locovei S, Dahl G. 2004; Pannexin membrane channels are mechanosensitive conduits for ATP. FEBS Lett. 572:65–68. [PubMed: 15304325]
14. Thi MM, Islam S, Suadicani SO, et al. 2012; Connexin43 and pannexin1 channels in osteoblasts: who is the "hemichannel"? J. Membr. Biol. 245:401–409. [PubMed: 22797941]
15. Pelegrin P, Surprenant A. 2006; Pannexin-1 mediates large pore formation and interleukin-1beta release by the ATP-gated P2X7 receptor. EMBO J. 25:5071–5082. [PubMed: 17036048]
16. Silverman WR, de Rivero Vaccari JP, Locovei S, et al. 2009; The pannexin 1 channel activates the inflammasome in neurons and astrocytes. J. Biol. Chem. 284:18143–18151. [PubMed: 19416975]
17. Locovei S, Bao L, Dahl G. 2006; Pannexin 1 in erythrocytes: function without a gap. Proc. Natl. Acad. Sci. U. S. A. 103:7655–7659. [PubMed: 16682648]
18. Li J, Liu D, Ke HZ, et al. 2005; The P2X7 nucleotide receptor mediates skeletal mechanotransduction. J. Biol. Chem. 280:42952–42959. [PubMed: 16269410]
19. Beckel JM, Argall AJ, Lim JC, et al. 2014; Mechanosensitive release of adenosine 5'-triphosphate through pannexin channels and mechanosensitive upregulation of pannexin channels in optic nerve head astrocytes: a mechanism for purinergic involvement in chronic strain. Glia. 62:1486–1501. [PubMed: 24839011]
20. Suadicani SO, Brosnan CF, Scemes E. 2006; P2X7 receptors mediate ATP release and amplification of astrocytic intercellular Ca2+ signaling. J. Neurosci. 26:1378–1385. [PubMed: 16452661]
21. Locovei S, Scemes E, Qiu F, et al. 2007; Pannexin1 is part of the pore forming unit of the P2X7 receptor death complex. FEBS Lett. 581:483–488. [PubMed: 17240370]
22. Negoro H, Urban-Maldonado M, Liou LS, et al. 2014; Pannexin 1 channels play essential roles in urothelial mechanotransduction and intercellular signaling. PLoS One. 9:e106269. [PubMed: 25170954]
23. Toft BR, Nordling J. 2006; Recent developments of intravesical therapy of painful bladder syndrome/interstitial cystitis: a review. Current opinion in urology. 16:268–272. [PubMed: 16770126]
24. Chekeni FB, Elliott MR, Sandilos JK, et al. 2010; Pannexin 1 channels mediate 'find-me' signal release and membrane permeability during apoptosis. Nature. 467:863–867. [PubMed: 20944749]
25. Orellana JA, Froger N, Ezan P, et al. 2011; ATP and glutamate released via astroglial connexin 43 hemichannels mediate neuronal death through activation of pannexin 1 hemichannels. J. Neurochem. 118:826–840. [PubMed: 21294731]
26. Santiago MF, Veliskova J, Patel NK, et al. 2011; Targeting pannexin1 improves seizure outcome. PLoS One. 6:e25178. [PubMed: 21949881]
27. Dvoriantchikova G, Ivanov D, Barakat D, et al. 2012; Genetic ablation of Pannexin1 protects retinal neurons from ischemic injury. PLoS One. 7:e31991. [PubMed: 22384122]

28. Gulbransen BD, Bashashati M, Hirota SA, et al. 2012; Activation of neuronal P2X7 receptor-pannexin-1 mediates death of enteric neurons during colitis. Nat. Med. 18:600–604. [PubMed: 22426419]
29. Lutz SE, Gonzalez-Fernandez E, Ventura JC, et al. 2013; Contribution of pannexin1 to experimental autoimmune encephalomyelitis. PLoS One. 8:e66657. [PubMed: 23885286]
30. Cheung WY, Fritton JC, Morgan SA, et al. 2016; Pannexin-1 and P2X7-Receptor Are Required for Apoptotic Osteocytes in Fatigued Bone to Trigger RANKL Production in Neighboring Bystander Osteocytes. J. Bone Miner. Res. 31:890–899. [PubMed: 26553756]
31. Penuela S, Gyenis L, Ablack A, et al. 2012; Loss of pannexin 1 attenuates melanoma progression by reversion to a melanocytic phenotype. J. Biol. Chem. 287:29184–29193. [PubMed: 22753409]
32. Bonewald LF, Johnson ML. 2008; Osteocytes, mechanosensing and Wnt signaling. Bone. 42:606–615. [PubMed: 18280232]
33. Baron R, Kneissel M. 2013; WNT signaling in bone homeostasis and disease: from human mutations to treatments. Nat. Med. 19:179–192. [PubMed: 23389618]
34. Burgers TA, Williams BO. 2013; Regulation of Wnt/beta-catenin signaling within and from osteocytes. Bone. 54:244–249. [PubMed: 23470835]
35. Robinson JA, Chatterjee-Kishore M, Yaworsky PJ, et al. 2006; Wnt/beta-catenin signaling is a normal physiological response to mechanical loading in bone. J. Biol. Chem. 281:31720–31728. [PubMed: 16908522]
36. Sawakami K, Robling AG, Ai M, et al. 2006; The Wnt co-receptor LRP5 is essential for skeletal mechanotransduction but not for the anabolic bone response to parathyroid hormone treatment. J. Biol. Chem. 281:23698–23711. [PubMed: 16790443]
37. Lau KH, Kapur S, Kesavan C, et al. 2006; Up-regulation of the Wnt, estrogen receptor, insulin-like growth factor-I, and bone morphogenetic protein pathways in C57BL/6J osteoblasts as opposed to C3H/HeJ osteoblasts in part contributes to the differential anabolic response to fluid shear. J. Biol. Chem. 281:9576–9588. [PubMed: 16461770]
38. Buckland J. 2015; Bone: Anabolic Wnt/beta-catenin signalling: osteocytes are key. Nature reviews. Rheumatology. 11:128.
39. Lara-Castillo N, Kim-Weroha NA, Kamel MA, et al. 2015; In vivo mechanical loading rapidly activates beta-catenin signaling in osteocytes through a prostaglandin mediated mechanism. Bone. 76:58–66. [PubMed: 25836764]
40. Hens JR, Wilson KM, Dann P, et al. 2005; TOPGAL mice show that the canonical Wnt signaling pathway is active during bone development and growth and is activated by mechanical loading in vitro. J. Bone Miner. Res. 20:1103–1113. [PubMed: 15940363]
41. Tu X, Delgado-Calle J, Condon KW, et al. 2015; Osteocytes mediate the anabolic actions of canonical Wnt/beta-catenin signaling in bone. Proc. Natl. Acad. Sci. U. S. A. 112:E478–486. [PubMed: 25605937]
42. Javaheri B, Stern AR, Lara N, et al. 2014; Deletion of a single beta-catenin allele in osteocytes abolishes the bone anabolic response to loading. J. Bone Miner. Res. 29:705–715. [PubMed: 23929793]
43. Kamel MA, Picconi JL, Lara-Castillo N, et al. 2010; Activation of beta-catenin signaling in MLO-Y4 osteocytic cells versus 2T3 osteoblastic cells by fluid flow shear stress and PGE2: Implications for the study of mechanosensation in bone. Bone. 47:872–881. [PubMed: 20713195]
44. Robling AG, Niziolek PJ, Baldridge LA, et al. 2008; Mechanical stimulation of bone in vivo reduces osteocyte expression of Sost/sclerostin. J. Biol. Chem. 283:5866–5875. [PubMed: 18089564]
45. Poole KE, van Bezooijen RL, Loveridge N, et al. 2005; Sclerostin is a delayed secreted product of osteocytes that inhibits bone formation. FASEB J. 19:1842–1844. [PubMed: 16123173]
46. van Bezooijen RL, ten Dijke P, Papapoulos SE, et al. 2005; SOST/sclerostin, an osteocyte-derived negative regulator of bone formation. Cytokine Growth Factor Rev. 16:319–327. [PubMed: 15869900]
47. Semenov M, Tamai K, He X. 2005; SOST is a ligand for LRP5/LRP6 and a Wnt signaling inhibitor. J. Biol. Chem. 280:26770–26775. [PubMed: 15908424]

48. Turner CH, Warden SJ, Bellido T, et al. 2009; Mechanobiology of the skeleton. Science signaling. 2:pt3. [PubMed: 19401590]
49. Hanstein R, Negoro H, Patel NK, et al. 2013; Promises and pitfalls of a Pannexin1 transgenic mouse line. Front. Pharmacol. 4:61. [PubMed: 23675350]
50. Zemel B. 2013; Bone mineral accretion and its relationship to growth, sexual maturation and body composition during childhood and adolescence. World Rev. Nutr. Diet. 106:39–45. [PubMed: 23428679]
51. Wallace JM, Rajachar RM, Allen MR, et al. 2007; Exercise-induced changes in the cortical bone of growing mice are bone- and gender-specific. Bone. 40:1120–1127. [PubMed: 17240210]
52. Raghavan M, Sahar ND, Kohn DH, et al. 2012; Age-specific profiles of tissue-level composition and mechanical properties in murine cortical bone. Bone. 50:942–953. [PubMed: 22285889]
53. Kennedy OD, Laudier DM, Majeska RJ, et al. 2014; Osteocyte apoptosis is required for production of osteoclastogenic signals following bone fatigue in vivo. Bone. 64:132–137. [PubMed: 24709687]
54. Xiong J, Onal M, Jilka RL, et al. 2011; Matrix-embedded cells control osteoclast formation. Nat. Med. 17:1235–1241. [PubMed: 21909103]
55. Thi MM, Urban-Maldonado M, Spray DC, et al. 2010; Characterization of hTERT-immortalized osteoblast cell lines generated from wild-type and connexin43-null mouse calvaria. Am. J. Physiol. Cell Physiol. 299:C994–C1006. [PubMed: 20686067]
56. Gupta RR, Yoo DJ, Hebert C, et al. 2010; Induction of an osteocyte-like phenotype by fibroblast growth factor-2. Biochem. Biophys. Res. Commun. 402:258–264. [PubMed: 20934405]
57. Hopfer U, Hopfer H, Meyer-Schwesinger C, et al. 2009; Lack of type VIII collagen in mice ameliorates diabetic nephropathy. Diabetes. 58:1672–1681. [PubMed: 19401424]
58. Seref-Ferlengez Z, Basta-Pljakic J, Kennedy OD, et al. 2014; Structural and Mechanical Repair of Diffuse Damage in Cortical Bone In Vivo. J. Bone Miner. Res. 29:2537–2544. [PubMed: 25042459]
59. Robling AG, Turner CH. 2002; Mechanotransduction in bone: genetic effects on mechanosensitivity in mice. Bone. 31:562–569. [PubMed: 12477569]
60. Dempster DW, Compston JE, Drezner MK, et al. 2013; Standardized nomenclature, symbols, and units for bone histomorphometry: a 2012 update of the report of the ASBMR Histomorphometry Nomenclature Committee. J. Bone Miner. Res. 28:2–17. [PubMed: 23197339]
61. Bonewald LF. 2011; The amazing osteocyte. J. Bone Miner. Res. 26:229–238. [PubMed: 21254230]
62. Seref-Ferlengez Z, Suadicani SO, Thi MM. 2016; A new perspective on mechanisms governing skeletal complications in type 1 diabetes. Ann. N. Y. Acad. Sci. 1383:67–79. [PubMed: 27571221]
63. Pacheco-Costa R, Atkinson E, Dilley JE, et al. 2017; Absence of pannexin-1 in osteocytes leads to high bone mass due to distinct cellular mechanisms in cancellous versus cortical bone, and in young versus old mice. J Bone Miner Res [Abstract]. 32(Suppl 1)
64. Adriouch S, Dox C, Welge V, et al. 2002; Cutting edge: a natural P451L mutation in the cytoplasmic domain impairs the function of the mouse P2X7 receptor. J. Immunol. 169:4108–4112. [PubMed: 12370338]
65. Suadicani SO, Iglesias R, Spray DC, et al. 2009; Point mutation in the mouse P2X7 receptor affects intercellular calcium waves in astrocytes. ASN Neuro. 1:55–63.

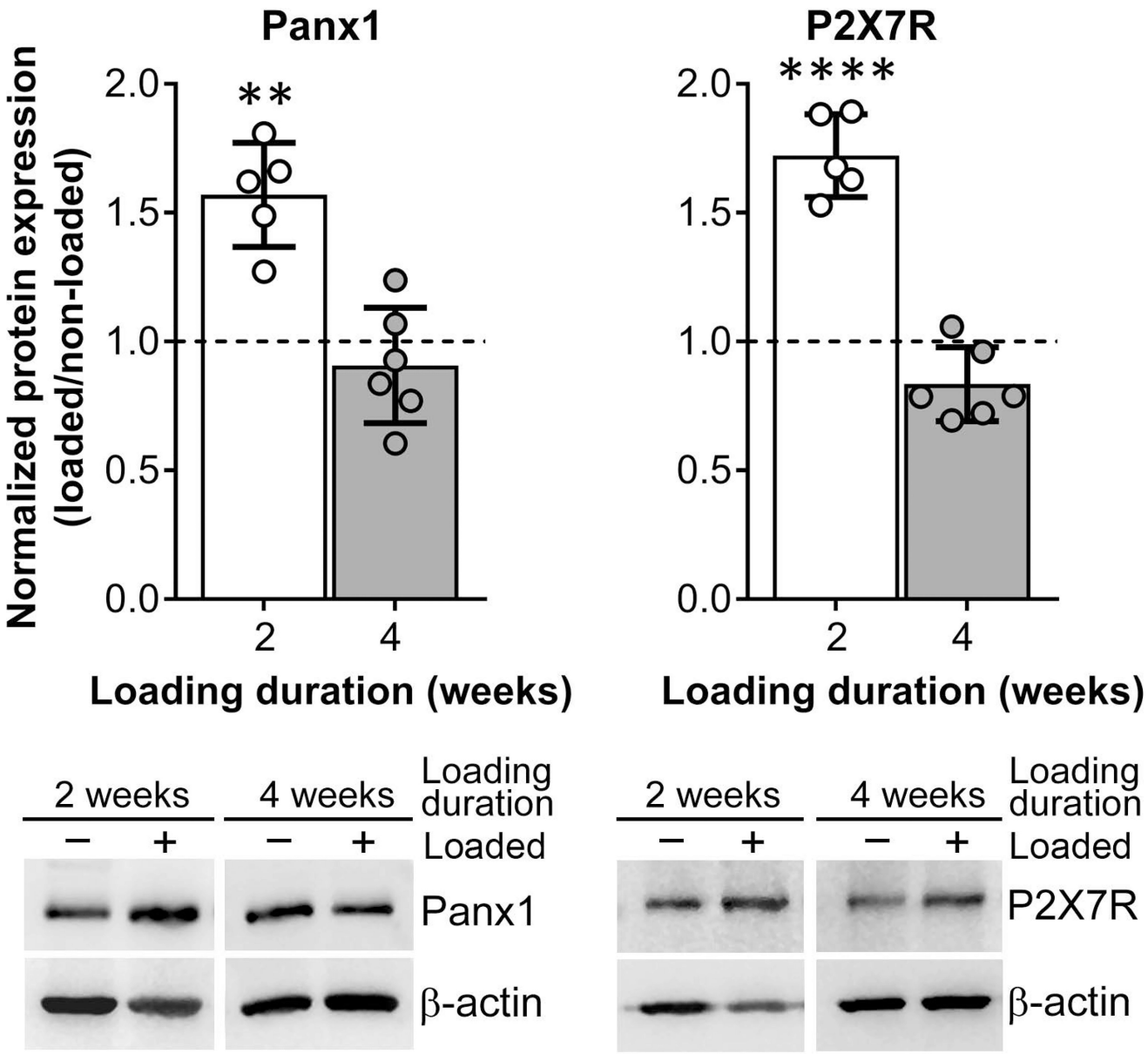

Figure 1.

The P2X7R-Panx1 mechanosignaling complex response to mechanical loading in wildtype mice is time dependent. Expression of Panx1 and P2X7R in loaded wildtype compared to age-matched non-loaded wildtype after 2 or 4 weeks of loading (treadmill running). Representative western blots for Panx1 and P2X7R from 2 weeks and 4 weeks loaded (positive symbol) and non-loaded controls (negative symbol) are shown below the graph. Protein levels were first normalized with the respective β-actin loading protein control, and then with the age-matched non-loaded wildtype levels. **P<0.01, ***P<0.001, non-loaded wildtype (dotted line) vs. age-matched loaded wildtype, nonparametric *t*-test followed by Mann-Whitney comparison test. Loading duration group: $n = 5$ (2 weeks), $n = 6$ (4 weeks). Data presented as means ± SD.

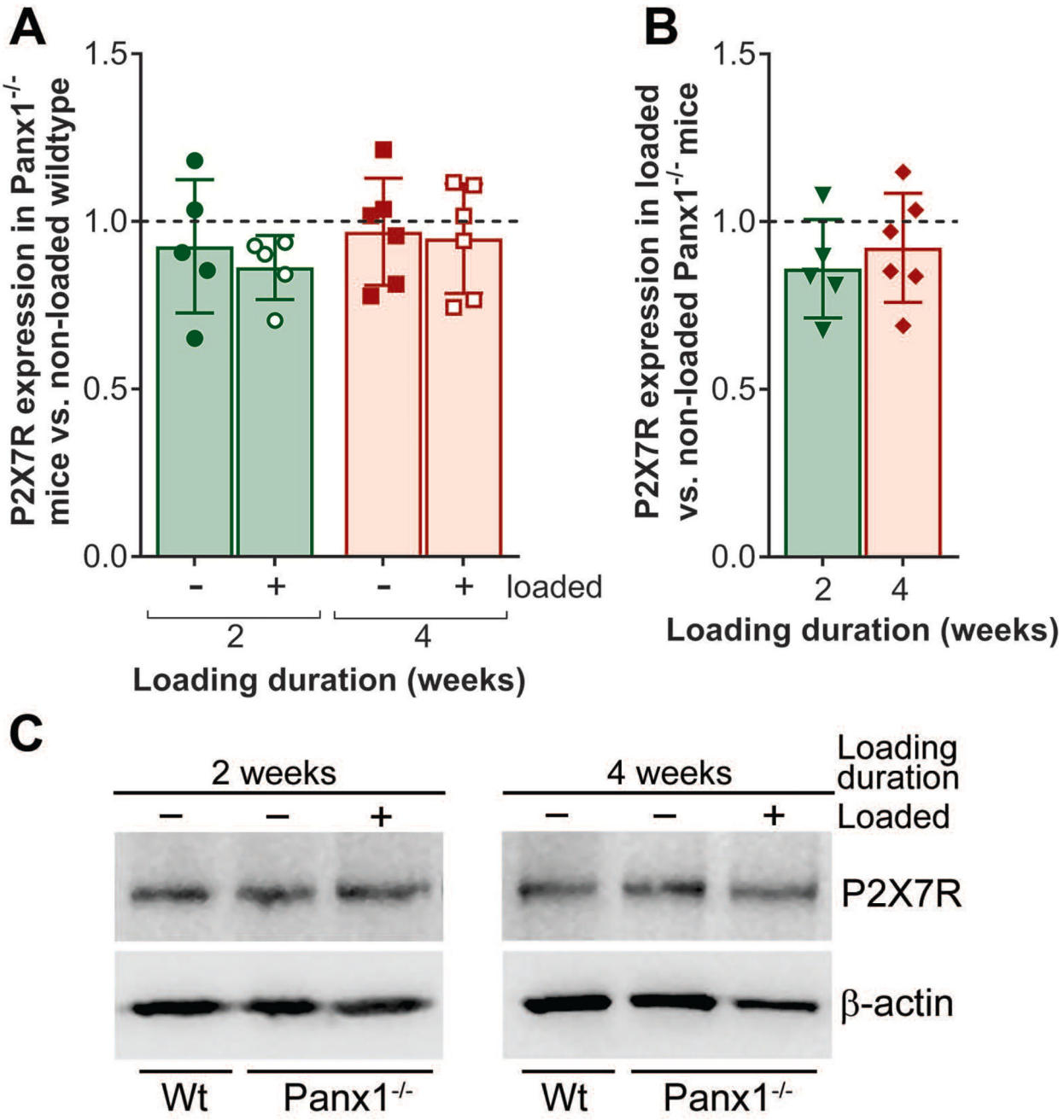

Figure 2.

P2X7R expression in response to mechanical loading in *Panx1*$^{-/-}$ mice. (A) Expression of P2X7R in non-loaded and loaded *Panx1*$^{-/-}$ compared to age-matched non-loaded wildtype (dotted line) after 2 or 4 weeks of loading (treadmill running). (B) Expression of P2X7R in loaded *Panx1*$^{-/-}$ compared to age-matched non-loaded *Panx1*$^{-/-}$ (dotted line) after 2 or 4 weeks of loading. (C) Representative western blots for P2X7R from 2 weeks and 4 weeks loaded *Panx1*$^{-/-}$ mice (positive symbol) and non-loaded age match controls (negative symbol). Protein levels were first normalized with the respective β-actin loading control, and then with the age-matched non-loaded wildtype levels. Comparisons were performed using

one-way ANOVA followed by Tukey's multiple comparison test. For the comparison between *Panx1*$^{-/-}$ non-loaded vs. age-matched loaded, an unpaired *t*-test was used followed by Mann-Whitney comparison test. Loading duration group: $n = 5$ (2 weeks), $n = 6$ (4 weeks). Data presented as means ± SD.

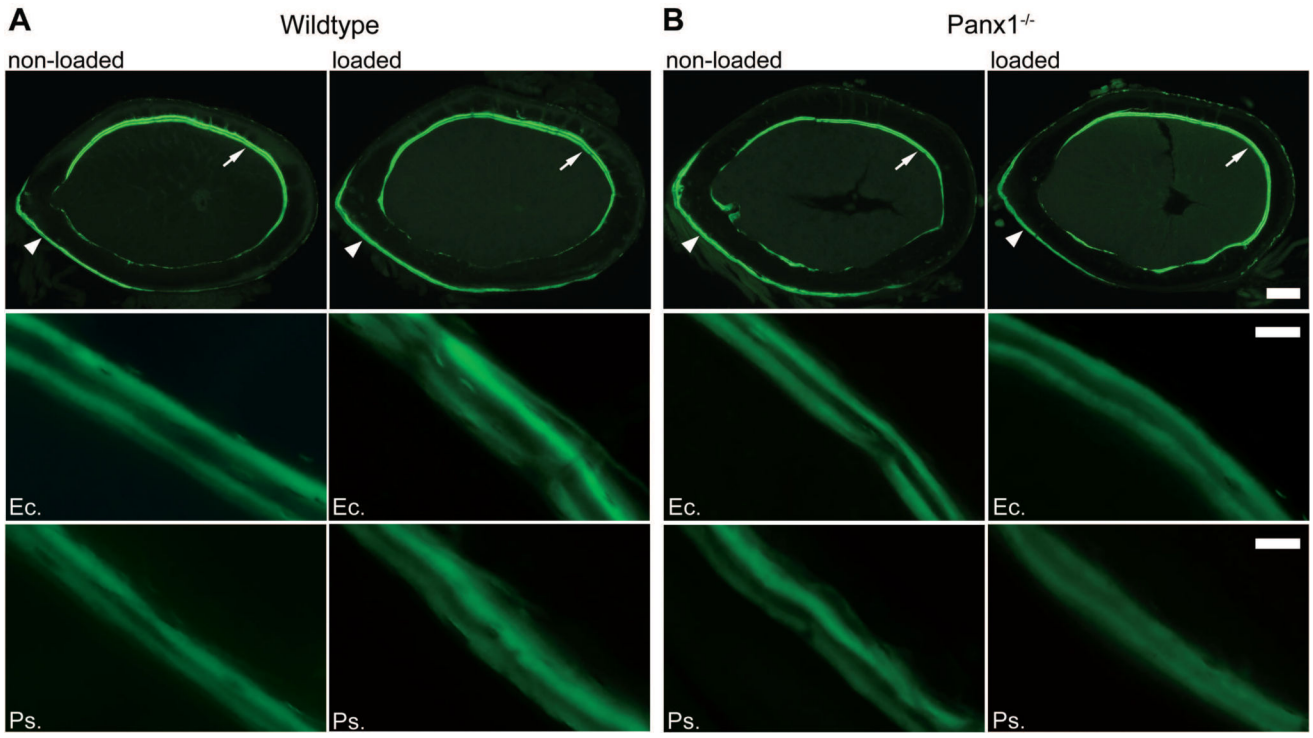

Figure 3.

Load-induced changes in the periosteal and endocortical surfaces of femoral midshaft after 2 weeks of loading in wildtype and *Panx1*$^{-/-}$ mice. Top panels: Representative cross-section images showing double calcein labels for age-matched non-loaded and loaded wildtype (A) and *Panx1*$^{-/-}$ (B) bones. Scale bar = 200 μm. Middle panels: Representative images of double calcein labeling on lateral endocortical (Ec.) surfaces (indicated with arrows in the top panels) of non-loaded and loaded wildtype and *Panx1*$^{-/-}$ bones. Scale bar = 20 μm. Bottom panels: Representative images of double calcein labeling on medial periosteal (Ps.) surfaces (indicated with arrowheads in the top panels) of non-loaded and loaded wildtype and *Panx1*$^{-/-}$ bones. Scale bar = 20 μm.

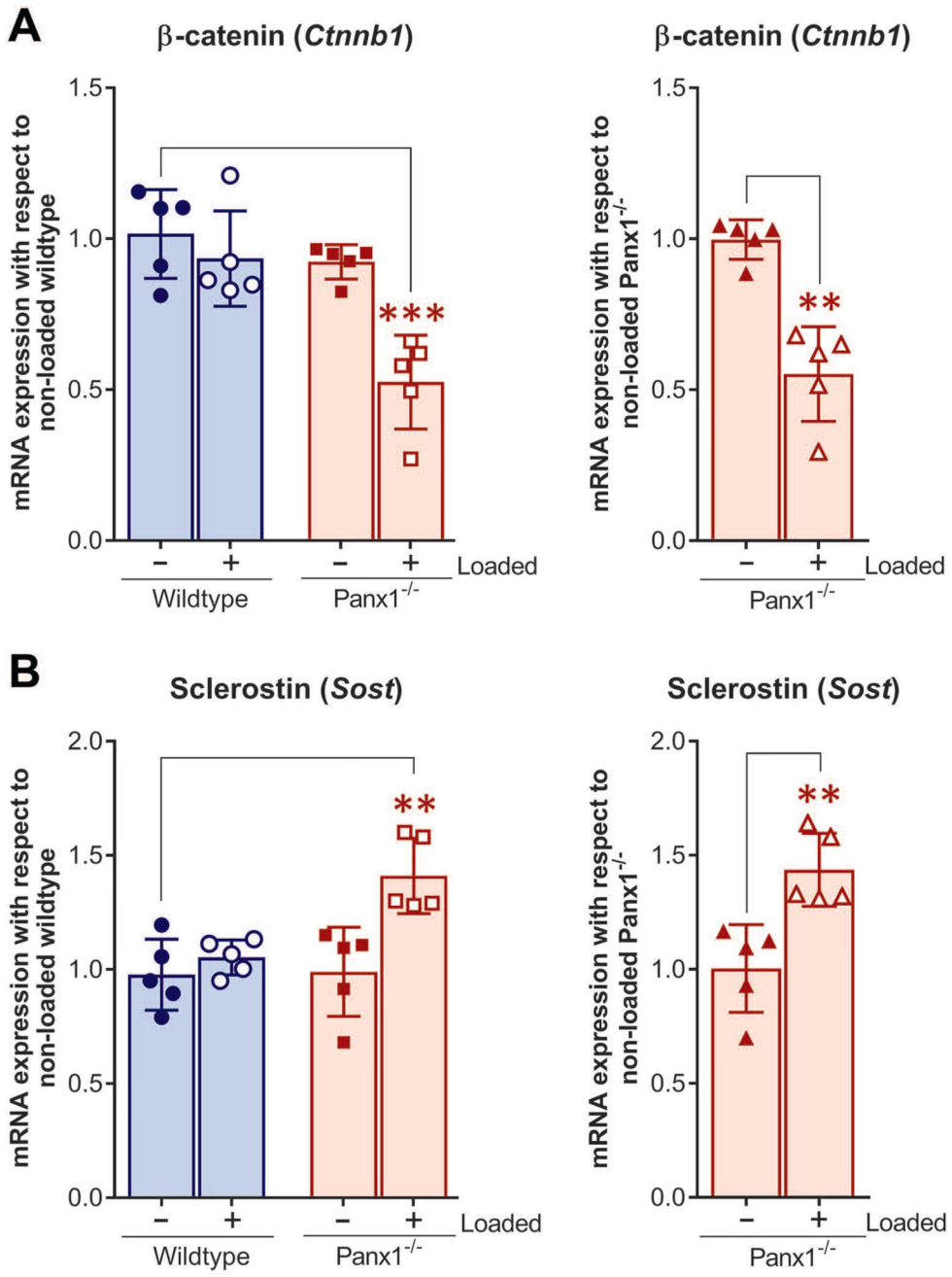

Figure 4.

mRNA expression of β-catenin and sclerostin after 4 weeks loading in wildtype and *Panx1*$^{-/-}$ mice. q-PCR analysis of (A) β-catenin (*Ctnnb1*) and (B) sclerostin (*Sost*) mRNA expression in loaded wildtype, loaded *Panx1*$^{-/-}$, and non-loaded *Panx1*$^{-/-}$ relative to age-matched non-loaded wildtype, and loaded *Panx1*$^{-/-}$ relative to age-matched non-loaded *Panx1*$^{-/-}$. The delta-delta CT method was used for data analysis, where the value obtained for each gene of interest is first normalized to the reference gene (18S rRNA gene) and then to either age-matched non-loaded wildtype or age-matched non-loaded *Panx1*$^{-/-}$. All data are presented as mean ± SD, $n = 5$; **P < 0.01, ***P < 0.001. P values were obtained using

either one-way ANOVA followed by Tukey's multiple comparison test or unpaired *t*-test followed by Mann-Whitney test.

Table 1

Histological studies showing load-induced changes in femoral midshaft of 4-week loaded vs. non-loaded wildtype and *Panx1*$^{-/-}$ bones.

Parameters	Wildtype		*Panx1*$^{-/-}$	
	non-loaded (*n* = 6)	loaded (*n* = 6)	non-loaded (*n* = 7)	loaded (*n* = 6)
Body weight (g)	28.8 ± 1.5	26.8 ± 2.08	26.3 ± 1.44	25.1 ± 2.02
Tt.Ar (mm^2)	1.71 ± 0.09			
Ct.B.Ar (mm^2)	0.76 ± 0.05			
Ct.B.Ar / Tt.Ar	0.45 ± 0.02	0.45 ± 0.04	0.48 ± 0.02	0.44 ± 0.02
Ma.Ar (mm^2)	0.94 ± 0.05		0.99 ± 0.04	0.96 ± 0.05
Ct.Th (μm)	194.1 ± 5	202.3 ± 16	206.2 ± 8	199.0 ± 16
***J* (mm^4)**	0.35 ± 0.03		0.41 ± 0.02	0.39 ± 0.07
I_x (mm^4)	0.12 ± 0.01		0.14 ± 0.01	0.13 ± 0.03
I_y(mm^4)	0.24 ± 0.02		0.27 ± 0.02	0.26 ± 0.04

*P<0.05,

**P<0.01, comparisons with respect to non-loaded wildtype using one-way ANOVA followed by Tukey's multiple comparison test.

$^{\#}$P<0.05, comparison between loaded vs. non-loaded *Panx1*$^{-/-}$ using unpaired *t*-test followed by Mann-Whitney test.

n = number of animals/group. Total area (Tt.Ar), cortical bone area (Ct.B.Ar), marrow area (Ma.Ar), cortical thickness (Ct.Th), polar moment of inertia (*J*) and area moment of inertia (I_X and I_Y) are presented as the means ± SD.

Table 2

Dynamic histomorphometric studies showing load-induced changes in femoral midshaft of 2-week loaded vs. non-loaded wildtype and *Panx1*$^{-/-}$ bones.

Parameters	Wildtype		*Panx1*$^{-/-}$	
	non-loaded (*n* = 5)	loaded (*n* = 5)	non-loaded (*n* = 4)	loaded (*n* = 4)
Ps.MS/BS (%)	17.5 ± 3.9		23.7 ± 4.9	
Ps.MAR (μm/day)	1.4 ± 0.2	1.6 ± 0.2	1.5 ± 0.1	1.3 ± 0.2
Ps.BFR/BS (μm^3/μm^2/day)	0.25 ± 0.1		0.34 ± 0.07	
Ec.MS/BS (%)	34.7 ± 8.7	32.9 ± 6.2	34.6 ± 4.9	40.1 ± 2.2
Ec.MAR (μm/day)	1.6 ± 0.4	1.6 ± 0.5	1.1 ± 0.3	1.4 ± 0.1
Ec.BFR/BS (μm^3/μm^2/day)	0.58 ± 0.3	0.53 ± 0.3	0.38 ± 0.13	0.56 ± 0.06

**P<0.01, comparisons with respect to age-matched non-loaded wildtype;

$^{\#}$P<0.05, loaded vs. age-matched non-loaded *Panx1*$^{-/-}$; one-way ANOVA followed by Tukey's multiple comparison test.

Periosteal mineralizing surface (Ps.Ms/Bs), periosteal mineral apposition rate (Ps.MAR), periosteal bone formation rate (Ps.BFR/BS), endocortical mineralizing surface (Ec.Ms/Bs), endocortical mineral apposition rate (Ec.MAR), and endocortical bone formation rate (Ec.BFR/BS) are presented as means ± SD.